J. Biochem. 2010;148(6):639–650 doi:10.1093/jb/mvq099

JB THE JOURNAL OF BIOCHEMISTRY

Dual role of the carboxyl-terminal region of pig liver L-kynurenine 3-monooxygenase: mitochondrial-targeting signal and enzymatic activity*

Received June 9, 2010; accepted August 23, 2010; published online August 27, 2010

Kumiko Hirai[1], Hidehito Kuroyanagi[2,†], Yoshitaka Tatebayashi[3], Yoshitaka Hayashi[3], Kanako Hirabayashi-Takahashi[4], Kuniaki Saito[4,‡], Seiich Haga[5], Tomihiko Uemura[6,7,§] and Susumu Izumi[7,¶]

[1]Neuronal Signaling Research Team, Tokyo Institute of Psychiatry, 2-1-8, Kamikitazawa, Setagaya-ku, Tokyo 156-8585; [2]Department of Molecular Genetics, Tokyo Metropolitan Institute of Gerontology, 35-2 Sakaecho, Itabashi-ku, Tokyo, 173-0015; [3]Depression Research Project Team, Tokyo Institute of Psychiatry, 2-1-8, Kamikitazawa, Setagaya-ku, Tokyo, 156-8585; [4]Department of Informative Clinical Medicine, Gifu University Graduate School of Medicine, 1-1, Yanagido, Gifu, 501-1194; [5]Schizophrenia Research Project Team, Tokyo Institute of Psychiatri, 2-1-8, Kamikitazawa, Setagaya-ku, Tokyo, 156-8585; [6]Tama Psychiatric Hospital, 2082 Nakano-cho, Hachioji-shi, Tokyo, 192-0015 and [7]Department of Biological Sciences, Division of Biochemistry, Tokyo Metropolitan University, 1-1 Minami-osawa, Hachioji-shi, Tokyo 192-0397, Japan

*This article is dedicated to the memory of Prof. Yashiro Kotake (1879–1968), a discoverer of kyunrenine, and in commemoration of the centennial anniversary of founding Department of Biochemistry, Osaka University.

†Present address: Hidehito Kuroyanagi, Department of Functional Genomics, Tokyo Medical and Dental University, Medical Research Institute and School of Biomedical Science, 1-5-45, Yushima, Bunkyo-ku, Tokyo, 113-8510.

‡Present address: Kuniaki Saito, Human Health Sciences, School of Medicine and Faculty of Medicine, Kyoto University, 53, Kawahara-cho, Shogoin, Sakyo, Kyoto 606-8507.

§Tomihiko Uemura, Tama Psychiatric Hospital, 2082, Nakano-cho, Hachioji-shi, Tokyo, 192-0015, Japan. Tel: +81 042 623 5308, Fax: +81 042 626 6218, email: t.uemura-perseo@river.ocn.ne.jp

¶Present address: Susumu Izumi, Department of Biological Sciences, Faculty of Science, Kanagawa University, Tsuchiya 2946, Hiratsuka-shi 259-1293, Japan.

L-kynurenine 3-monooxygenase (KMO) is an NAD(P)H-dependent flavin monooxygenase that catalyses the hydroxylation of L-kynurenine to 3-hydroxykynurenine, and is localized as an oligomer in the mitochondrial outer membrane. In the human brain, KMO may play an important role in the formation of two neurotoxins, 3-hydroxykynurenine and quinolinic acid, both of which provoke severe neurodegenerative diseases. In mosquitos, it plays a role in the formation both of eye pigment and of an exflagellation-inducing factor (xanthurenic acid). Here, we present evidence that the C-terminal region of pig liver KMO plays a dual role. First, it is required for the enzymatic activity. Second, it functions as a mitochondrial targeting signal as seen in monoamine oxidase B (MAO B) or outer membrane cytochrome b_5. The first role was shown by the comparison of the enzymatic activity of two mutants (C-terminally FLAG-tagged KMO and carboxyl-terminal truncation form, KMOΔC50) with that of the wild-type enzyme expressed in COS-7 cells. The second role was demonstrated with fluorescence microscopy by the comparison of the intracellular localization of the wild-type, three carboxyl-terminal truncated forms (ΔC20, ΔC30 and ΔC50), C-terminally FLAG-tagged wild-type and a mutant KMO, where two arginine residues, Arg461-Arg462, were replaced with Ser residues.

Keywords: Carboxyl-terminal truncation/hydrophobic C-terminal domain/L-kynurenine 3-monooxygenase/mitochondrial targeting signal/mitochondrial tail-anchored protein.

Abbreviations: BCIP, 5-bromo-4-chloro-3-indolyl phosphate; ER, endoplasmic reticulum; GAPDH, D-glyceraldehyde-3-phosphate dehydrogenase; KMO, L-kynurenine 3-monooxygenase; 3-HK, 3-hydroxykynurenine; mAb, monoclonal antibody; MAO B, monoamine oxidase B; MOM, mitochondrial outer membrane; MW, molecular weight; NBT, nitrobluetetrazolium chloride; OM b_5, outer membrane cytochrome b_5; ORF, open reading frame; PHBH, *p*-hydroxybenzoate hydoxylase; PVDF, polyvinylidene difluoride; TBS, tris-buffered saline; TMD, transmembrane domain; 3D structure, three-dimensional structure.

L-kynurenine 3-monooxygenase (KMO, EC1.14.13.9) is an oligomeric protein that contains 1 mol of non-covalently bound FAD/mol of monomeric enzyme (*1*). KMO localizes in the mitochondrial outer membrane (MOM) (*2*). It belongs to the family of external monooxygenase (*3*) and is widely distributed in non-neural tissues and cell lineages, such as liver, kidney, macrophages, microglia, monocytes (*4*–*6*) and is present also, although in low amount, in the central nervous system (*7*, *8*). Two neurotoxins are formed from kynurenine; 3-hydroxykynurenine (3-HK) from kynurenine by KMO and quinolinic acid from HK by an additional three steps, *i.e.* kynureninase acting on HK, 3-hydroxyanthranilate 3,4-dioxygenase and autocyclization (*9*).

HK is a more potent neurotoxin than qunolinic acid (*10*, *11*) and is elevated in acute immune activation (*12*), transient cerebral ischemia (*13*), HIV-1-infection with dementia (*14*), hepatic encephalopathy (*15*),

Parkinson's disease (*16*), Huntington's disease (*17*) and in plasma of haemodialysed patients (*18*). The aim of the present work is to obtain novel information on the regions of the protein involved in its activity and localization because of the importance of this enzyme under cerebral pathophysiological conditions.

In this article, we report the functional expression of cDNA encoding pig KMO in COS-7 cells. Analysis of deletion mutants showed that the segment of 20 amino acid residues (positions from −30 to −50 from C-terminus) was necessary for the enzymatic activity while a double-substitution mutant analysis showed that two arginine residues, R461 and R462, within the C-terminal 20 amino acid sequence were necessary for the targeting of KMO to MOMs. Previous studies had not revealed a role of the C-terminal portion of KMO in its enzymatic activity although it has been reported that the C-terminal 32 amino acids portion of MAO B is important both for membrane binding and for stability of the enzyme (*19*). Thus, the C-terminal region of KMO enzyme couples the role of a targeting signal to the MOM with that of maintaining the enzymatic activity.

Experimental Procedures

Construction of various KMO derivatives

We constructed the KMO derivatives starting from a pig KMO cDNA (1-1,438-bp fragment). This cDNA fragment was amplified by PCR with the primers shown on the first line of Table I. The amplified fragment was digested with *Xho I* and *Kpn I*, and subcloned into the *Sal I* and *Kpn I* sites of the expression vector, pFLAG-CMV-5a (Eastman Kodak Company).

FLAG-free KMO and deletion mutants of KMO were constructed by the manipulation of KMO cDNA and named so that the numbers of the truncated residues were indicated. The employed sense and anti-sense primer sequences are shown in Table I. The deleted constructs were checked by sequencing and the amplified KMO cDNAs were digested and inserted as above at the site of *Sal I* and of *Kpn I* into pFLAG-CMV-5a vector pre-treated with calf intestinal alkaline phosphatase. Alternatively, FLAG-free KMO (RR type and SS type) were also constructed by digesting the amplified fragment with *Not I* and *Kpn I* and subcloning into the *Not I* and *Kpn I* sites of the expression vector, pcDNA3.1 (+/−) (Invitrogen). In this case, primers used for PCR are shown in Table II and template DNAs used are cDNA (RR type) or cDNA (SS type), respectively (*vide infra*).

A double substitution mutant (SS type) was constructed by substitution of both arginines at positions 461 and 462 with serine residues. The employed forward and reverse primer sequences are shown in Table I. The components for PCR were Pyrobest buffer, 0.2 mM dNTP, 30 pmol of each primer, 400 pg of template DNA and 5 U of Pyrobest DNA Polymerase (TaKaRa Biomedicals) in a final volume of 100 µl. Thermal cycling conditions were 94°C for 5 min followed by 25 cycles (94°C, 30 s; 63.7°C 30 s; 72°C, 5–7 min in a final cycle). The purified blunt-end PCR product (210 ng) was phosphorylated with 20 U of T4 polynucleotide kinase and 2 mM ATP in a final volume of 100 µl, purified, self-ligated with Ligase Kit I (TaKaRa DNA Ligation Kit Ver. S), and it was used for transformation of competent *Escherichia coli* (DH5-α) by the method of (*20*). After isolation of Bluescript plasmids carrying the cDNA inserts, they were submitted to DNA sequencing to verify the exact substitution. The cDNA coding for the double-substitution mutant was sub-cloned into the *Pst I* and *Kpn I* site of the expression vectors, pCMV-5a and pFLAG-CMV-5a. They were transfected by the Lipofectamine method (*21*) into COS-7 cells which were maintained in Dulbecco's modified Eagle's medium supplemented with 10% foetal bovine serum and penicillin (100 U/ml)–streptomycin (100 µg/ml) in an atmosphere of 5% CO_2.

Western blot analysis

KMO derivatives expressed in COS-7 cells were detected by western blots. SDS–PAGE was carried out on a 10% gel or on a 12% gel. After electrophoresis, proteins were horizontally transferred onto polyvinylidene difluoride (PVDF) membrane. Marker proteins were stained with Ponceau S or a rainbow marker (Amersham, High Range) was occasionally used. The other part of the membrane was incubated with tris-buffered saline (TBS) containing 2% BSA overnight. The blot was incubated with anti-KMO monoclonal antibody (mAb) 7C1 (*1*) (1 : 2000) or anti-FLAG mAb M2 (Sigma, 1 : 300) for 2 h, with alkaline phosphatase-conjugated goat anti-mouse IgG (Stratagene, 1 : 5,000) for 1 h, rinsed with TBS containing 0.05% Tween-20, and developed with 5-bromo-4-chloro-3-indolyl phosphate (BCIP)/nitrobluetetrazolium chloride (NBT) (Stratagene) for 10 min. D-Glyceraldehyde-3-phosphate dehydrogenase (GAPDH) band detected with anti-GAPDH (Santa Cruz Biotechnology, 1 : 2,000) was used as housekeeping gene-derived protein to check the probable toxic effect of transfected plasmids on COS-7. The intensity of the stained bands was

Table II. Primers used for PCR.

Primers	
Sense	5′-aaaa*ggtacc*gccaccATGAAAAACACCTCGGCG GTGATGG-3′ from 5 to 29 nt
Anti-sense	5′-aaaa *gcggccgc*TTACAGGGAGATGCGTCCTA TAT-3′ from 1419 to 1441 nt

Added restriction sites (*Kpn I* and *Not I*) are in small letter and italic. Stop codon is underlined with a solid line.

Table I. Primers used for PCR.

FLAG-KMO and KMO Mutants	Sense primers	Anti-sense primers
FLAG-tagged KMO	5′-CCG*CTCGAG*AATTA TGAAAAACACCTCG GC-3′ from 1 to 21 nt	5′-GC*GGTACC*CAGGGAGATGCGTCCTATATTTTG-3′ from 1415 to 1438 nt
FLAG-free KMO	The same as above	5′-GC*GGTACC*GTTTTGGTCACTGAGAAATCA-3′ from 1516 to 1536 nt
KMOΔC10D	The same as above	5′-CCG*GGTACC*TTTAAGTGACCGAGTTCCATGA-3′ from 1391 to 1408 nt
KMOΔC20D	The same as above	5′-CCG*GGTACC*TTTAGCCCAGGGAGCTCCGAAA-3′ from 1361 to 1378 nt
KMOΔC30D	The same as above	5′-CCG*GGTACC*TTTAAAGGAGGTAGGTGGTGCT-3′ from 1331 to 1348 nt
KMOΔC50D	The same as above	5′-CCG*GGTACC*TTTACACCTTTTTTTGCCATTG-3′ from 1271 to 1288 nt
KMOΔC70D	The same as above	5′-CCG*GGTACC*TTTAAACCATGGTATAGAGAGG-3′ from 1211 to 1228 nt
$KMOR_{461}SR_{462}S$	5′-GAGCAGCTCATGG AACTCGGTCAC-3′ from 1384 to 1407 nt	5′-AAGCAGCCCAGGGAGCTCCGAAAC-3′ from 1360 to 1383 nt

Added restriction sites (*Xho I* and *Kpn I*) are in italic. Added stop codon is underlined with a solid line.

quantified densitometrically using National Institutes of Health Image Software or Lumi-Imager F1 (Roche-diagnostics) with LumiAnalyst Soft. Enzyme activity of expressed KMO derivatives was normalized for differences in stained band intensity. We electrophoresed purified KMO solely as a molecular weight (MW) marker and not for the estimation of exact quantity of KMO (*vide infra*, Enzyme assay and Fig. 2a).

Enzyme assays

KMO activities of COS-7 cells transfected with various KMO derivatives were determined as follows: the reaction mixture consisted of ~4 μg COS-7 cell homogenates, 0.1 M Tris–acetate buffer (pH 8.0), 0.006% Triton X-100, 0.01 M KCl, 5 mM $MgCl_2$, 50 μM FAD, 1.5 mM NADPH, 5 mM glucose-6-phosphate, 3.5 U glucose-6-phosphate dehydrogenase and 0.3 mM L-kynurenine in a final volume of 600 μl and was incubated for 10 min at 37°C. 3-HK formed was measured by an HPLC-ECD (*7*). Each activity per milligram of COS-7 cell homogenate protein was statistically analysed by Student's *t*-test using Stat View (Macintosh version, SAS Institute Inc.). In order to make the comparison of the activities among the KMO derivatives, we quantified the amounts of each KMO derivative expressed in cell homogenates by the intensity of each KMO band on the western blotting (*vide sopra*) because almost equal amount of protein (20 μg) was loaded in each well on the assumption that mAb could stain equally any KMO mutants even C-terminally truncated forms. The activity was corrected comparing the western-blot band intensity among wild-type and KMO mutants *i.e.* a ratio of band intensity of KMO derivatives to that of wild-type was calculated and we multiplied each ratio by the corresponding activity. Protein was measured by DC protein microassay kits (Bio-Rad) with BSA as the standard.

Immunofluorescence microscopy

For conventional fluorescent microscopy, COS-7 cells were grown on coverslips in Multi Well Plate with 24 wells and transfected with 500 ng of plasmid DNAs using Lipofectamine 2000 reagent (Life Technologies, Inc.) according to the manufacture's instructions. Twenty-four to forty-eight hours after transfection, cells on the coverslips were stained for mitochondria with Mitotracker CMV Ros (Molecular Probes, Inc.) as described by De Silvestris *et al.* (*22*). After incubation with the dye for 30 min in the CO_2 incubator, cells were fixed with 4% paraformaldehyde for 10 min, permeabilized with 0.1% Triton X-100 for 2 min and processed for fluorescent immunostaining. We used anti-KMO mAbs 4F9 or 7C1 (1 : 2,000) as previously reported (*1*). Cells were analysed initially by standard fluorescence microscopy (Nikon Microphoto-FXA microscope equipped for epifluorescence). For confocal fluorescent microscopy, cells were grown to 70% confluency in eight well Lab-Tek chambers and transfected with 500 ng of KMO cDNAs (wild-type RR, double-substituted SS type or their FLAG-attached forms). Twenty-four hours after transfection, cells were fixed, permeabilized, processed for fluorescent immunostaining as above using anti-KMO mAb 7C1 (1 : 4,000) or mAb against FLAG (1 : 500, Sigma) and analysed with a Zeiss laser confocal microscope (LSM5 Pascal). CS2 (Adobe System Inc.) was used for image processing.

Results

Multiple sequence alignment of pig liver KMO with the proteins from four species

We isolated a 1.6-kb cDNA clone coding for pig liver KMO having an open reading frame (ORF) of 478 amino acids with a predicted molecular mass of 54.7 kDa and have deposited the sequence in the GenBank Data Libraries (accession number AF163971).

Figure 1A shows the predicted amino acid sequence of pig KMO with a multiple alignment with those of human (*23*), rat (Genbank accession number AF05631), yellow fever (*24*) and malaria mosquitos (*25*) KMO. The first ATG codon (nucleotides 5–7) in pig KMO is conserved neither in human (*23*) nor in rat KMO cDNA and the second ATG codon (nucleotides 26–28) in pig KMO is consistent with human (nucleotides 53–55) and rat (*45–47*) KMO initiation codon. Both initiation codon (nucleotides 5–7 and 26–28) in pig KMO fulfill the Kozak's consensus sequence (*26*) and KMO constructed in the present study from the deposited sequence showed good enzymatic activity (*vide infra*). Amino acid sequences of pig (*Sus scrofa*) KMO showed 82 and 44% identities with those of human (*Homo sapiens*) and mosquito (*Aedes aegypti*) KMO (*24*), respectively. Three shadowed areas are well conserved among five species and even in NADPH-dependent flavin monooxygenase (*p*-hydroxybenzoate hydoxylase, PHBH) from *Pseudomonas fluorescens* (*27*). The first shadowed area (GXGXXG motif) with the hydrophobic amino acid residues (position 18, 20, 31, 34, 41 and 43 in pig KMO, *i.e.* I, V, A, L, V and V, respectively, shown by triangles in Fig. 1A) is indispensable for the correct folding of the βαβ-structure of the dinucleotide-binding domain, the second area is a part of a site serving putative dual function in FAD/NADPH binding and the third area corresponds to a short part of the binding site for the riboflavin moiety of FAD (*28*). Figure 1B shows the C-terminal 53 amino acid sequence of the pig liver KMO protein and Fig. 1C shows the hydropathy plot of whole pig liver KMO protein. We can see the presence of a relatively short hydrophobic regions (shown by shadow in Fig. 1B and by box in Fig. 1A, respectively) that could function as a transmembrane domain (TMD) common to five species; this domain is flanked on both sides by positively charged residues that could act as the targeting signal to the MOM (*29*, *30*). In mosquito KMO, however, only one lysine residues is present upstream to the TMD, and the two downstream arginine residues are substituted with serine. In mammalian KMO, the two downstream arginine residues are generally conserved except in rat in which the latter arginine is substituted with serine (Fig. 1A). The C-terminus of pig KMO has a hydrophobic amino acid stretch previously noticed for human KMO but it has not been decided whether these relatively hydrophobic regions are responsible for mitochondial anchoring or not (*23*).

Construction of KMO mutants and their expression in COS-7 cells detected by western-blot analysis

To analyse the roles of C-terminal region of KMO, various mutations were introduced into the pig KMO C-terminal region (Scheme 1). The mutants were introduced into COS-7 cells and their expression was detected by western blot analysis. As shown in Fig. 2A, anti-KMO mAb 7C1 detected a purified KMO of 49 kDa which was included as a marker (see also *1*). Practically no KMO protein band was seen in the mock transfected cells (Fig. 2A) or in untransfected (Fig. 2B) COS-7 cells. Similarly, it has been reported that COS-7 cells do not contain MAO B protein (*31*). Proteins with similar mobility were found in the lysates of COS-7 cells transfected with wild-type KMO and KMO deletion mutants, ΔC10D, ΔC20D and ΔC30D (Fig. 2A). Transfected wild-type KMO moved slightly faster than the marker-purified KMO. The reason for this minor difference in mobility is not

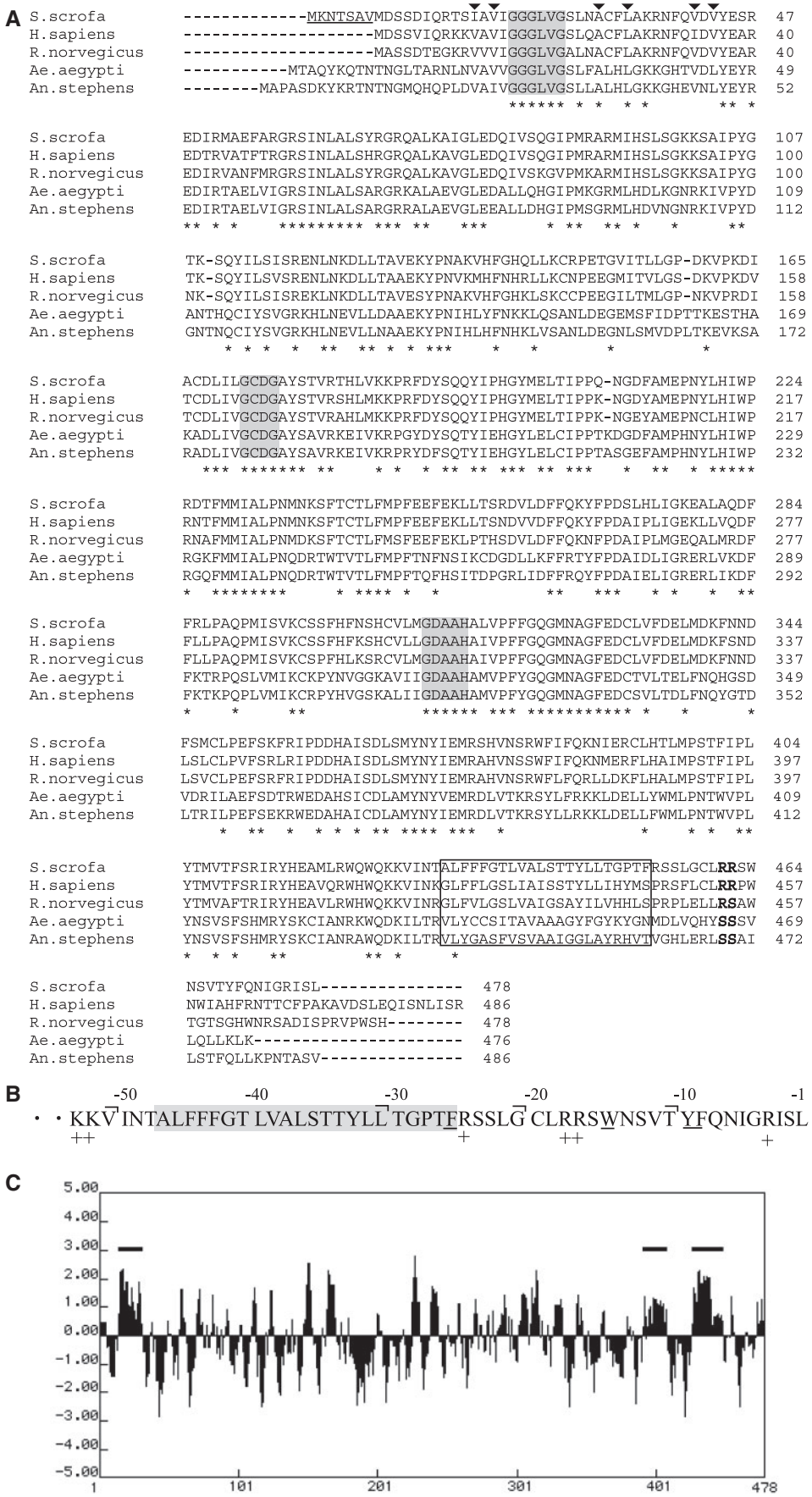

Fig. 1 (A) Multiple sequence alignment of pig liver KMO with the proteins from four species. The amino acid sequences were aligned by the CLUSTAL method. Amino acids identical in all five KMOs are indicated by an asterisk. The hydrophobic amino acid residues required for the correct fold of the βαβ-structure of the dinucleotide-binding domain in pig KMO are marked by inverse filled triangle. The seven N-terminal

Continued

known presently. It is possible that exoproteolysis at the N- and/or C-terminus removed a few animo acid residues. Alternatively, the protein purified from liver and the one expressed in cells could differ in some post-translational modification. Protein bands with faster mobility were detected for ΔC50D and ΔC70D. The faster mobility presumably reflects the smaller molecular size predicted from the ORF rather than a degradation process, since ΔC70D migrated ahead of ΔC50D. The absence of a mobility shift in ΔC10D, ΔC20D and ΔC30D was unexpected, since the lack of amino acids in the C-terminal region of these mutants was confirmed by DNA sequencing of the constructs. In the case of MAO B, similar deletions cause the expected mobility shifts (*19*). Presently we have no explanation for this abnormal mobility but the different content of hydrophobic amino acids between KMO and MAO B in this C-terminal region might be one reason. KMO-FLAG moved slightly slower than wild-type KMO probably due to the attachment of FLAG. Anti-FLAG mAb detected a protein only in the transfectant with KMO-FLAG (Fig. 2A, middle part).

The intensities of KMO protein bands in lysates from cells expressing the ΔC10D and ΔC20D mutants were similar to that of the wild-type KMO. In contrast, the intensity of the protein band in cell lysates expressing the ΔC30D mutant was ~30% higher than that of the wild-type, while those in ΔC50D and ΔC70D mutants were lower (58–68% of the wild-type). It is likely that the anti-KMO mAb 7C1 exhibited similar immunoreactivity toward every KMO mutants, although the epitope of the mAb was not yet determined. Hence, the difference in band intensities in various mutants might reflect their expression levels in COS-7 cells.

The GAPDH bands of COS-7 cells transfected with various plasmids were also analysed. As shown in Fig. 2A, lower panel, GAPDH bands were of essentially identical intensity in transfected, mock transfected and non-transfected cells (Fig. 2B, left lane), indicating no toxic effect of KMO plasmid transfections on COS-7 cells.

Enzyme activity of transfected COS-7 cells with Pig KMO cDNA

The corrected KMO activities of the homogenates of cells transfected with various KMO derivatives are shown as relative ratio (%) to that of wild-type KMO (Fig. 3). The homogenates of transfectants with wild-type KMO showed a specific activity of 2,010 ± 31 pmol/min/mg COS-7 cell homogenate protein ($n = 3$), whereas mock transfectants exhibited <10% of the wild type. A K_m value for L-kynurenine was ~16 μM (data not shown), comparable to the reported K_m value of the partially purified rat liver enzyme (*32*) and of the transiently expressed human enzyme (*23*). KMO-FLAG showed ~30% lower activity than wild-type KMO (Fig. 3) despite similar expression levels (Fig. 2A), suggesting that the FLAG sequence at the carboxyl-terminus may have some effect on the enzymatic activity.

Two forms of carboxyl-terminal truncation, KMOΔC10D and KMOΔC20D retained almost full activity but KMOΔC30D showed 1.6-fold higher activity than the wild-type. The quantity of expressed KMOΔ30D was 1.3-fold higher than the wild-type KMO (Fig. 2A), so the 1.6-fold significantly higher activity could not be explained by the quantity of expressed KMO alone. We think that not only the expressed quantity but also the quality of the C-terminal 30 truncated enzyme may favour the hydroxylation of L-kynurenine. KMOΔC50D and KMOΔC70D, however, lost the activity by >90% compared with the wild-type (Fig. 3). The much lower activity could not be explained by lower expression alone (Fig. 2A) since the quantity of the expressed C-terminally deleted ΔC50D was 58–66% and that of the ΔC70D was 68% of the wild-type enzyme. In other words, both deleted enzymes showed only ~30–40% less expression than the wild-type enzyme in spite of <10% of the activity (Fig. 3). Therefore, the very low activity could not be explained only by the lower quantity of the expressed enzyme. The KMO mutant SS type showed ~40% lower specific activity than wild RR type KMO (Fig. 3). This is consistent with the observation that wild-type KMO of *A. stephensi* which lacks the two Arg residues of the mammalian enzyme, is very unstable and looses its activity just after purification (*25*).

Mitochondrial targeting signal of KMO

A net positive charge at the C-terminus is essential for mitochondrial targeting for many C-terminally anchored membrane proteins (*29*, *30*), *e.g.* three positively charged amino acids within its carboxyl-terminal 29 amino acid residues for MAO B (*33*), two positively charged amino acids within the carboxyl-terminal 10 amino acid residues for OM b_5 (*34*) and four basic amino acids within its carboxyl-terminal 32 amino acid residues for Fis 1 (*35*). KMO has four basic amino acids and four aromatic amino acids within the C-terminal 29 amino acid residues (Fig. 1B). We analysed by immunofluorescence microscopy the sub-cellular localization of various KMO derivatives.

Fig. 1 Continued
amino acids in pig KMO not conserved in human and rat are underlined. The first-shadowed area is a consensus sequences associated with a binding site to the ADP portion of FAD, the second is a part of the FAD/NADPH-binding site and the third is a part of the binding site of the ribityl moiety of FAD. All three areas are strictly conserved also in bacterial PHBH. Bold letters indicate amino acid substitutions for the Arg residues in position 461 and 462 in variants R461S R462S which are seen in the wild-type enzyme of two mosquitos. A putative transmembrane hydrophobic domain in all five KMOs is boxed. Genebank accession numbers: *Aedes aegypti*, AA027576; *Anopheles stephensi*, AAL 40890; *Homo sapiens*, NP_003670; *S. scrofa*, AF163971; *Ratus norvegicus*, AF056031 (B) C-terminal amino acid sequence of pig liver KMO. Residues are numbered from the C-terminus with negative numbers. Positions of deletion are marked with '¬'. Within the C-terminal 29 amino acid residues, positively charged amino acids are shown by plus and aromatic amino acids are underlined. A putative transmembrane hydrophobic domain is highlighted in grey. Two positively charged amino acids upstream to the TMD are also shown by plus. (C) Kyte-Doolittle hydopathy plot for KMO. Window setting = 7. Three considerably hydrophobic segments are shown by thick lines.

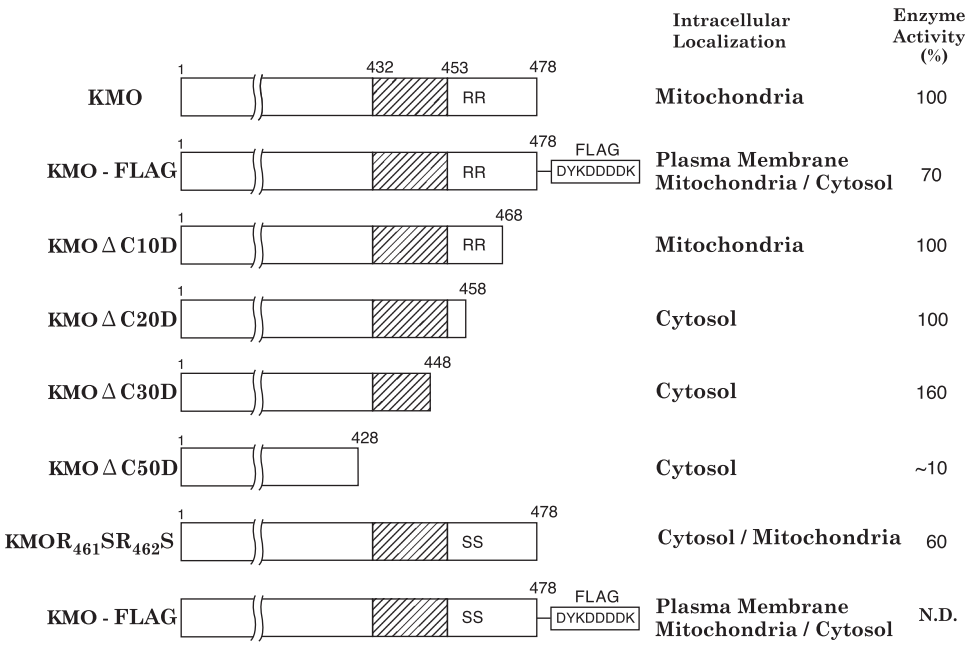

Scheme 1 Schematic representation of KMO constructs, subcellular localization and their enzymatic activity. The numbers shown above the bars are the positions of amino acids in each protein. The hatched portions indicate the predicted transmembrane hydrophobic domain. The enzymatic activity of FLAG-attached SS form was not determined (N.D.).

KMO had a staining pattern compatible with that of mitochondria (*36*) where a dot-like structure was seen both in the perinuclear area and in the periphery of the cells (Fig. 4A-a and -b) similar to those of MAO B (*33*) and OM b_5 (*34*). The staining around the nucleus may correspond to autophagic vacuoles seen at yet higher levels of expression as shown in the case of OM b_5 (*34*). In contrast, KMO-FLAG showed two distinct stained compartments: one was a punctuate-stained structure (Fig. 4A-d) overlapping with mitochondrial staining (Fig. 4A-c); the other was an area not corresponding to mitochondrial staining but rather spread out through the cytoplasm reaching the plasma membrane (Fig. 4A-d), suggesting that FLAG-tagged KMO fails to precisely target the MOM, presumably because the negatively charged FLAG sequence weakens the mitochondrial targeting signal. The partial localization of KMO-FLAG on plasma membrane was confirmed by laser confocal microscopy (*vide infra*).

Cells expressing KMOΔC10D showed a string- or dot-like structure (Fig. 4, Fig. 4A-e) like that of wild-type KMO (Fig. 4A-b). In contrast, KMOΔC20D and KMOΔC30D yielded diffuse cytoplasmic staining (Fig. 4A-f and -g), suggesting that their sub-cellular localizations are cytosolic like MAO B ΔC28D (*33*).

Since KMO-FLAG (Fig. 4A-d) did not exclusively localize to the mitochondrial OM, KMO, KMO (SS), KMO-FLAG and KMO (SS)-FLAG staining were reexamined by laser confocal microscopy (Fig. 4B). Cells transfected with a double substitution SS-type mutant, a natural form of the enzyme found in two species of mosquito (Fig. 1A), showed a mainly cytosolic staining pattern with some mitochondrial staining (Fig. 4B-2a and -c). This staining pattern is different from the RR wild-type staining pattern, which was clearly mitochondrial (Fig. 4B-1a). On the other hand, the staining pattern of wild-type KMO-FLAG, was spread out through the cytoplasm, reaching the plasma membrane with a few dot-like structure (Fig. 4B-3a). KMO-FLAG stained by anti-FLAG mAb (Fig. 4B-3d) showed diffuse cytoplasmic staining including the plasma membrane. Probably the enzyme was partially mistargeted to the endoplasmic reticulum (ER), and from there, travelled to the cell surface. Such an occurrence has been reported for a mutated form of cytochrome b_5, carrying an extended hydrophobic anchor lengthened by 5 amino acids (extended type cytochrome b_5 having total length of 22 amino acid residues like KMO) (*37*). The staining pattern of KMO (SS)-FLAG, *i.e.* FLAG-tagged SS-type mutant KMO, was more spread out through the cytoplasm and on the cell surface (Fig. 4B-4a) than that of KMO-FLAG (Fig. 4B-3a) and vesicular intracellular membranes superimposed on the mitochondrial staining were also seen (Fig. 4B-4c, merged image). KMO (SS)-FLAG stained by anti-FLAG mAb showed again intra-cellular plus cell surface staining (Fig. 4B-4d). Without FLAG, neither wild-type KMO (RR) (Fig. 4B-1d) nor KMO (SS) (Fig. 4B-2d) stained with anti-FLAG mAb.

Thus, FLAG attached to the C-terminus of KMO may weaken not only the positive charge but also the C-terminal hydrophobicity, both of which provoke unfavourable effects on mitochodrial targeting. These results suggest a critical role of a net positive charge of R461 and R462 for mitochondrial targeting. A similar example of the importance of two arginines at the C-terminus for mitochondrial localization has been reported using two constructed mutants, cytochrome b_5-RR and b_5-R. The former showed a clear mitochondrial localization and the latter showed a dual ER plus OM localization (*38*).

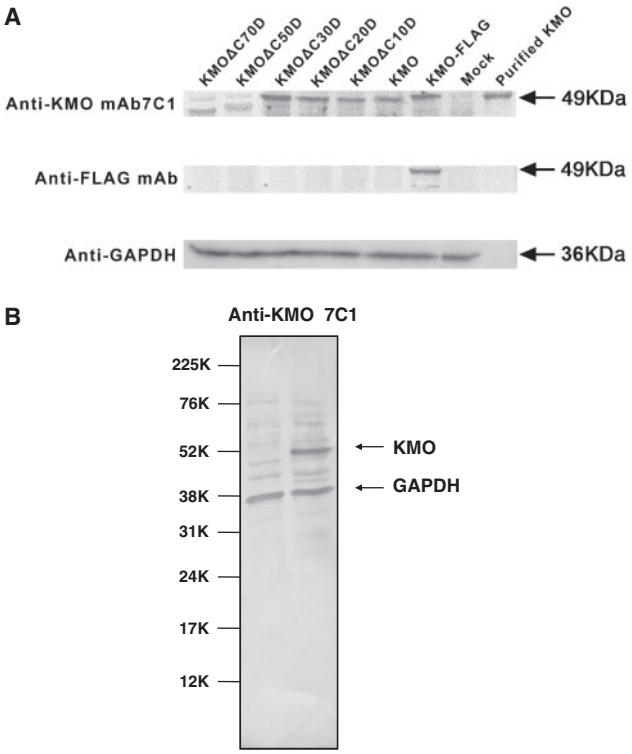

Fig. 2 (A) Western-blot analysis of purified and transiently expressed wild-type, FLAG-attached KMO and deletion mutants. COS-7 cells expressing the wild-type and mutant proteins of KMO were harvested, centrifuged and resuspended in SDS–PAGE sample buffer. Purified pig liver KMO (3.6 μg) or cell lysate (~20 μg) obtained from transfectants were electrophoresed and western-blot analyses were performed as described in 'Experimental Procedures' section. Note that the faster moving KMO band for KMOΔC50D and that for KMOΔC70D were less intensely stained than the others. (B) Comparison of non-transfected COS-7 cells and KMO cDNA transfected COS-7 cells. Left: non-transfected COS-7 cell; right: KMO cDNA transfected COS-7 cells. No staining of KMO in non-transfected COS-7 cells is detected. Numbers on the left indicate the position and size (kDa) of markers. Staining intensity of the GAPDH band for each lane was the same.

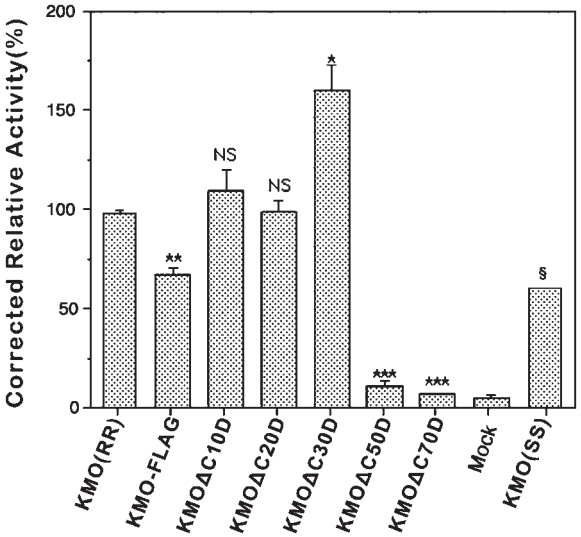

Fig. 3 Enzymatic activity of KMO derivatives expressed in COS-7 cells. The thawed cell homogenate was diluted 10-fold with 0.25 M sucrose (2 mM Tris–HCl buffer, pH 7.5) and 40 μl (~40 μg of protein) was used in a final reaction volume of 600 μl. The bar graphs depict the means ± S.E.M. of three independent experiments except for KMO-FLAG which was assayed in six independent experiments and for the mutant SS form, which was measured only once. 100% = 2,010 ± 31 pmol/min/mg COS-7 cell homogenate protein ($n = 3$). Each enzymatic activity was corrected by the expressed protein KMO band intensity determined by western blot as described in 'Experimental Procedures' section. $^{*}P < 0.02$; $^{**}P < 0.001$; $^{***}P < 0.0001$. [§]Only one experiment; NS, not significant.

Although our immunofluorescence data strongly suggest a mitochondrial localization for wild-type KMO protein, the localization of a small amount of KMO protein on mitochondria-associated ER membranes cannot be ruled out. Mitochondria-associated ER membranes function in lipids (*39*) and proteins (*40*) transport from the ER to mitochondria and KMO requires lipid factor(s) for its enzymatic activity (*41*). In fact, it was very difficult to demonstrate clear mitochondrial OM localization at slightly higher levels of expression (data not shown). The above described results (intra-cellular localization and enzymatic activity) are summarized in Scheme 1.

Discussion

We present, here, for the first time the finding that the C-terminal region is absolutely necessary for the enzymatic activity of KMO, as demonstrated by the loss in enzymatic activity of the two deletions, ΔC50D and ΔC70D (Fig. 3), which was greater than the reduction in immunostaining in western blot. It cannot be excluded that our mAb binds less efficiently to the C-terminally truncated forms and that consequently higher amounts of the mutants were expressed than assessed by western blotting. If this were the case, the extent of the reduction in enzyme activity of the truncated mutants would be even greater than the value calculated from the ratio of activity to western blot band intensity (western blot band intensity 64–76% of wild type versus the activity <10%) (Fig. 3). Further analysis revealed that the ΔC30D truncated-mutant retained full (rather higher) enzyme activity. Therefore, we can safely conclude that the sequence from −30 to −50 from the C-terminus is required for KMO enzyme activity.

Our result with KMO differs strikingly with results of similar studies on MAO B. In the latter enzyme, the carboxyl-terminal end is essential for interaction with the OM but not directly involved in the catalytic activity (*19*). While proceeding with the work, we took notice of the report on the presence in the yellow fever mosquito, *A. aegypti* (*24*) of a natural deletion mutant (ΔC54D) having no enzymatic activity similar to our ΔC50D form. A deletion of 162 nucleotides in the kh^{w} product of kh^{w}-mutant strains results in a loss of 54 amino acids which provokes disruption of the α-helical structure in the carboxyl-terminal region of the protein and loss of the enzymatic activity resulting in the *A. aegypti* white-eye mutant strain. Our results are thus consistent with the phenotype caused by the natural deletion form of the mutant mosquito. It will be of great interest to investigate whether a similar

deletion mutant is present in natural populations of another species of mosquito, the malaria vector, *A. stephensi*, from which cDNA cloning of KMO has been reported (*25*).

Our cloned and expressed wild-type KMO exhibited good enzyme activity (Fig. 3) although it presumably contains seven additional amino acid residues at the N-terminus (position 1–7 in pig KMO, *i.e.* MKNTSAV underlined in Fig. 1A) in comparison to the sequence registered in the database (SwissProt accession number Q9MZS9 gives a 471 amino acid polypeptide of 54.0 kDa). We include the first initiation site in our constructs, since the first AUG triplet (if within the Kozak consensus) is generally used as initiation codon in eukaryotic cytoplasma (*42*); the produced protein is predicted to contain 478 amino acids (Fig. 1A). However, we cannot exclude that both initiation sites, or only the second one, were used in the transfected cells, since we might not have resolved a difference of seven amino acids on our gels. Alternative translation initiation products may be targeted to different intracellular compartments (*43*). Since KMO ΔN15D (lacking the first 15 residues) showed a typical mitochondrial pattern of fluorescence and retained almost the same activity as wild type (data not shown), we conclude that the N-terminal region does not contain any targeting information, which resides instead exclusively in the C-terminal region (Figs 1B and 4A and B).

FAD and/or NADPH-binding sites near the N-terminus (see the second-shadowed area in Fig. 1A) and the binding motif for the ribityl moiety of FAD seen at about two-thirds of the amino acid sequence (see the third-shadowed area in Fig. 1A) are presumably essential for the hydroxylation catalyzed by KMO, but a stretch of 20 amino acid residues from C-terminus (positions from −30 to −50, see Fig. 1B) is also required for the enzymatic activity. The C-terminal 30 truncated mutant, *i.e.* KMOΔ30D, although in the cytosol (Fig. 4A-g), showed an enzymatic activity superior to that of wild type (Fig. 3), indicating that relocation to the cytosol of the ΔC50D and ΔC70D mutants is not the cause of the reduced catalytic activity. Such an example of the C-terminal domain truncated form being more active than wild type has been reported for cystathionine-β-synthase (in this case, post-translational modification) (*44*). Recently soluble-cytosolic KMO from *P. fluorescens* (*pf*KMO) purified without any detergent has been reported and it shows a very high-specific activity of ∼3,150–5,900 nmol O_2 consumed/min/mg protein (*45*), of the same order of magnitude of our purified pig liver mitochondrial KMO (4,495 nmol/min/mg protein) (*1*). Thus, KMO does not require membrane anchorage for its activity.

To span the membrane, an α-helical hydrophobic domain must be at least 21 residues in length (*46*). Alberati-Giani *et al.* proposed that the C-termius of human KMO, which contains relatively hydrophobic regions, may be responsible for mitochondrial anchoring (*23*). Here we presented evidence that one of three hydrophobic segments (Fig. 1C) located at residues 432–453 (see the shadowed area in Fig. 1B), which fulfills well Eisenberg's proposal (*46*), is required for anchoring since its deletion resulted in dislocation of the mutant enzyme to the cytosol. In addition, two Arg residues downstream to the hydrophobic sequence were also essential for correct targeting to mitochondria. Thus, the hydrophobic C-terminus appears to have a dual role, in targeting/membrane insertion and in the enzymatic activity (Fig. 3). What could be the molecular basis of the latter function?

Despite the relatively low homology (only 13% identity) between KMO and bacterial NADPH-dependent flavoprotein hydroxylase, PHBH (*47*), three domains important in enzyme function are highly conserved among KMO and PHBH. (i) GXGXXG (residues 22–27 in pig KMO), the dinucleotide-binding motif; (ii) GCDG (residues 172–175 in pig KMO), a part of FAD/NADPH binding site; and (iii) GDAAH (residues 310–314 in pig KMO), a part of the ribityl-binding motif (see Fig. 1A). The three-dimensional structure (3D structure) of PHBH has been solved, and a model of KMO generated by homology with PHBH has been used to identify a putative binding pocket for a potent selective competitive inhibitor of the enzyme (*47*). The model shows that the α-helical C-terminal domain essential to the enzymatic activity (see Fig. 3 and *24*) is not projected into the proposed active site as seen in PHBH. The carboxyl-terminal portion of PHBH serves as the interface between subunits whose interaction is a largely hydrophobic and non-covalent to form a dimer and finally an oligomer (*48*). Native KMO is an oligomer having very high-specific activity (*1*) but how the monomer assembles into a dimer and finally into an oligomer has not been considered for KMO and is a subject for future studies. It is tempting to speculate that the membrane anchoring hydrophobic stretch is involved in oligomer assembly. Similarly, our interpretation for the lower activity of FLAG-tagged KMO compared to the wild-type (Fig. 3) is that weakening the hydrophobicity due to the attached FLAG at the carboxyl terminus might disturb a tight interaction between each subunit to form a dimer. Although a beautiful 3D structure of human MAO B showing the C-terminal helices rooted into the lipid membrane bilayer has been presented (*49*), no information is available on dimer (or oligomer) formation mediated by the hydrophobic C-terminal portion.

During purification of KMO from pig liver mitochondrial OM, the enzyme preparation was always accompanied by two other outer membrane proteins, *i.e.* OM b_5 and MAO B, and it was very difficult to remove contamination by these two proteins (*1*). Furthermore, KMO has a relatively short TMD flanked by basic amino acids, upstream (K426 and K427) and downstream (four arginine residues, notably, two consecutive arginines, R461 and R462) (Fig. 1B), which fulfills well the requirement for the specific targeting of tail-anchored proteins to the OM (*29*, *30*, *50*). In rat, however, R462 is substituted by serine (Fig. 1A). No immunofluorescence studies on the intra-cellular localization of rat KMO have been reported so far, whereas a previous cell fractionation study, aimed at characterizing the sub-mitochondrial

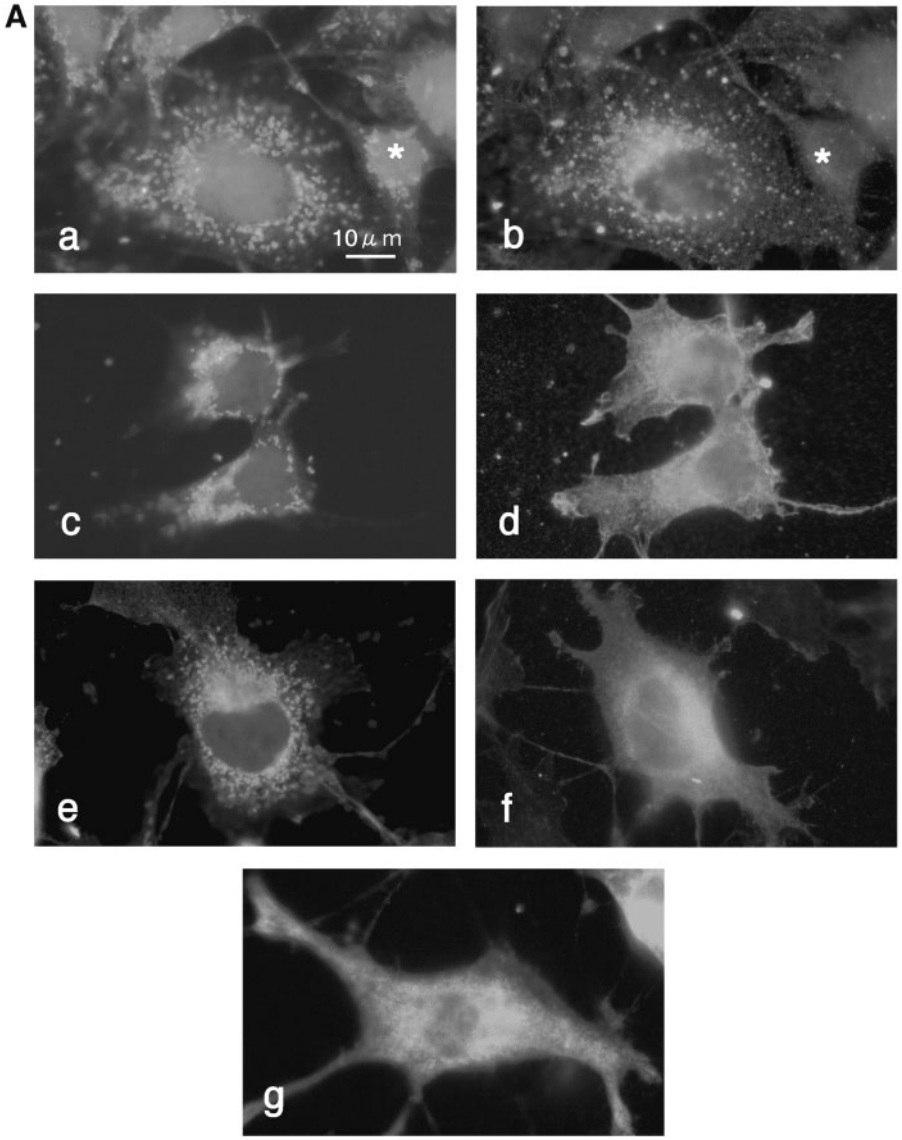

Fig. 4 Sub-cellular localization of KMO, KMO-FLAG, three deletion mutants and a double-substitution mutant in COS-7 cells observed by immunofluorescence. COS-7 cells were transiently transfected with non-tagged KMO cDNA, FLAG-tagged KMO cDNA or three deletion mutant cDNAs and then incubated with Mitotracker CMX Ros (250 nM) for 30 min, fixed, permeabilized and immunostained for KMO. (A) Conventional epifluorescence microscopy. The pairs (a) and (b), and (c) and (d) correspond to the same field of cells, respectively. (a) and (c) were viewed for mitochondria using the rhodamine filter, while (b) and (d) for KMO using the fluorescein filter. (a) and (b), non-tagged KMO; (c) and (d), FLAG-tagged KMO. The asterisk in (a) and (b) indicates a cell that either is non-transfected or expresses very low levels of KMO. (e), (f) and (g) show FITC-staining patterns for three deletion mutants, KMOΔC10D, KMOΔC20D, and KMOΔC30D, respectively. Note that (b) and (e) show a string or dot-like punctate stain, a typical mitochondrial pattern of fluorescence, with perinuclear-staining region, while (d) shows diffuse intracellular staining reaching the plasma membrane superimposed on the string- or dot-like pattern, suggesting a triple localization of the protein in mitochondria, cytosol and plama membrane. (f) and (g) show diffuse staining, suggesting the localization of the protein in the cytoplasm. (B) Confocal fluorescent microscopy. (*1*) and (*2*), Wild RR type and mutant SS type KMO (untagged), respectively; (*3*) and (*4*), FLAG-tagged wild RR type and mutant SS type KMO, respectively. Images of the same field were acquired sequentially with FITC (a) and Mitotrocker (b). (c) shows merged images of the two acquisitions. Single-confocal sections are shown. Anti-KMO mAb 7C1 (1 : 4,000) and goat anti-mouse FITC-labelled IgG secondary antibodies (1 : 1,000) were used. Scale bars: (*1*,*3*,*4*), 10 μm; (*2*), 20 μm. Note that non-tagged SS-mutant form (2a–2c) shows mainly cytosol staining with some mitochondrial staining, while FLAG-tagged SS-mutant form (4a and 4c), like the FLAG-tagged RR wild-type KMO (3a and 3c), shows intra-cellular vesicular membrane staining and a part of the protein reaches to the cell surface showing the margin of spikes (4d).

localization of KMO, showed that ~50% of the mitochondrial activity was recovered in the OM fraction (*2*). On the basis of the sequence of the rat KMO and considering the importance of two arginines at the C-terminus for precise anchoring in the MOM, one might predict that the rat enzyme has a dual localization (MOM plus cytosol or ER).

From our results and from the sequence analysis, we propose that KMO belongs to a family of outer membrane tail-anchored proteins like OM b_5 (*29*, *30*, *34*, *51*), Fis 1 (*35*), MAO B (*19*, *33*, *49*), VAMP-1b (*52*) and Bcl-xL (*53*). Four distinct functions of the tail-anchor domain were identified for Fis I (*35*). The first (the targeting to mitochondria) and the second

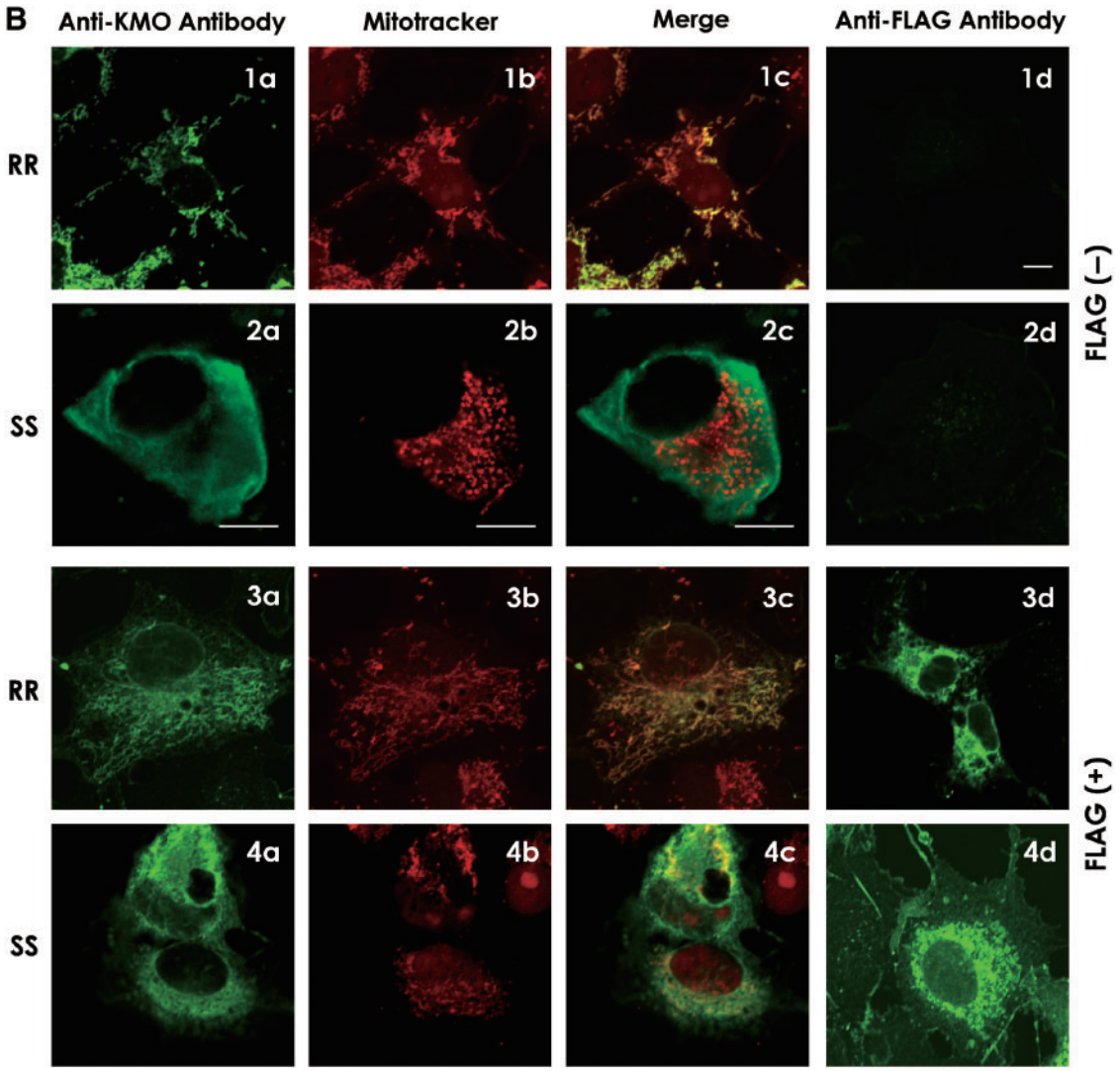

Fig. 4 (Continued).

(the insertion into the OM) are shared with KMO. The third function is that the tail-anchor is responsible for the assembly of the respective protein into functional multi-subunit complexes and the fourth function is their stabilization (*35*). Our results on the role of the C-terminal domain of KMO in its enzyme activity indirectly suggest that KMO's tail anchor carries out also the third role described for Fis I. However, further work is required to validate this hypothesis.

Acknowledgements

We thank Dr T. Shirasawa, Tokyo Metropolitan Institute of Gerontology and Medical Research Institute, Juntendo University for help in the initial period of the study of cDNA cloning, Dr N. Borgese, National Research Council Institute for Neuroscience and Department of Medical Pharmacology, University of Milano and Department of Pharmacological Science, University of Catanzaro 'Magna Graecia', Italy, for helpful discussion and for critically reading the article, Emeritus Prof. Y. Komano, Tokyo Metropolitan University, for fruitful discussions. Dr F. Kametani, Tokyo Institute of Psychiatry, Molecular Neurobiology Research Team for densitometrical analysis of band intensity. We thank the following Drs, Tokyo Metropolitan University, S. Hisanaga, A. Asada, for their generous gifts of COS-7 cells and Dr H. Tomaru in Unitech Company (Chiba, Japan) where part of the construction of FLAG-free KMO and its subcloning into pcDNA3.1 (+/−) were performed. We are grateful to Y. Shoda, E. Matsui and K. Suzuki for photographic assistance. T.U. obtained study opportunities from 2005 to 2007 of the long-term special register adult student system at graduate school of Tokyo Metropolitan University introduced from 2002 by Japanese Ministry of Education, Culture, Sports, Science and Technology.

Conflict of interest

None declared.

References

1. Uemura, T. and Hirai, K. (1998) L-Kynurenine 3-monooxygenase from mitochondrial outer membrane of pig liver: purification, some properties and monoclonal antibodies directed to the enzyme. *J. Biochem.* **123**, 253–262
2. Okamoto, H. and Hayaishi, O. (1967) On the submitochondrial localization of L-kynurenine-3-hydroxylase. *Biochem. Biophys. Res. Commun.* **26**, 309–314
3. Okamoto, H. and Hayaishi, O. (1967) Flavin adenine dinucleotide requirement for kynurenine hydroxylase of

rat liver mitochondria. *Biochem. Biophys. Res. Commun.* **29**, 394–399
4. De Castro, F.T., Brown, R.R., and Price, J.M. (1957) The intermediary metabolism of tryptophan by cat and rat tissue preparations. *J. Biol. Chem.* **28**, 777–784
5. Heyes, M.P., Saito, K., and Markey, S.P. (1992) Human macrophages convert L-tryptophan into the neurotoxin quinolinic acid. *Biochem. J.* **283**, 633–635
6. Heyes, M.P., Achim, C.L., Wiley, C.A., Major, E.O., Saito, K., and Markey, S.P. (1996) Human microglia convert L-tryptophan into the neurotoxin quinolinic acid. *Biochem. J.* **320**, 595–597
7. Uemura, T. and Hirai, K. (1991) Kynurenine 3-monooxygenase activity of rat brain mitochondria determined by high performance liquid chromatography with electrochemical detection in *Kynurenine and Serotonin Pathways*. (Schwarcz, R., Young, S.N., and Brown, R.R., eds.), pp. 531–534, Plenum Press, NY
8. Saito, K., Quearry, B.J., Saito, M., Nowak, T.S. Jr, Markey, S.P., and Heyes, M.P. (1993) Kynurenine 3-hydroxylase in brain: species activity differences and effect of gerbil cerebral ischemia. *Arch. Biochem. Biophys.* **307**, 104–109
9. Hayaishi, O. (1980) From oxygenase to superoxygenase in *Ogygen and Life, Second BOC Priestley Conference*, pp. 199–218, The Royal Society of Chemistry Burligton House, London. W1V 0BN
10. Nakagami, Y., Saito, H., and Katsuki, H. (1996) 3-Hydroxykynurenine toxicity on the rat striatum in vivo. *Jpn. J. Pharmacol.* **71**, 183–186
11. Okuda, S., Nishiyama, N., Saito, H., and Katsuki, H. (1998) 3-Hydroxykynurenine, an endogenous oxidative stress generator, causes neuronal cell death with apoptotic features and region selectivity. *J. Neurochem.* **70**, 299–307
12. Heyes, M.P., Quearry, B.J., and Markey, S.P. (1989) Systemic endotoxin increases L-tryptophan, 5-hydroxyindoleacetic acid, 3-hydroxykynurenine, and quinolinic acid content of mouse cerebral cortex. *Brain Res.* **491**, 173–179
13. Saito, K., Nowak, T.S. Jr, Makey, S.P., and Heyes, M.P. (1993) Mechanism of delayed increases in kynurenine pathway metabolism in damaged brain regions following transient cerebral ischemia. *J. Neurochem.* **60**, 180–192
14. Sardar, A.M., Bell, J.E., and Reynolds, G.P. (1995) Increased concentrations of the neurotoxin 3-hydroxykynurenine in the frontal cortex of HIV-1-positive patients. *J. Neurochem.* **64**, 932–935
15. Pearson, S.J. and Reynolds, G.P. (1991) The determination of 3-hydroxykynurenine in human brain and plasma by high performance liquid chromatography with electrochemical detection. Increased concentrations in hepatic encephalopathy. *J. Chromatogr. (Biomed. Appl.)* **565**, 436–440
16. Ogawa, T., Matson, W.R., Beal, M.F., Myers, R.H., Bird, E.D., Milbury, P., and Saso, S. (1992) Kynurenine pathway abnormalities in Parkinson's disease. *Neurology* **42**, 1702–1706
17. Reynolds, G.P. and Pearson, S.J. (1989) Increased brain 3-hydroxykynurenine in Huntington's disease. *Lancet* **ii**, 979–980
18. Pawlak, D., Pawlak, K., Malyszko, J., Mysliwiec, M., and Buczko, W. (2001) Accumulation of toxic products degradation of kynurenine in hemodialyzed patients. *Int. Urol. Nephrol.* **33**, 399–404
19. Rebrin, I., Geha, R.M., Chen, K., and Shih, J.C. (2001) Effects of carboxyl-terminal truncations on the activity and solubility of human monoamine oxidase B. *J. Biol. Chem.* **276**, 29499–29506
20. Inoue, H., Nojima, H., and Okayama, H. (1990) High efficiency transformation of *Escherichia coli* with plasmids. *Gene* **96**, 23–28
21. Loeffler, J. Ph, Barthel, F., Feltz, P., Behr, J.P., Sassone-Corsi, P., and Feltz, A. (1990) Lipopolyamine-mediated transfection allows gene expression studies in primary neuronal cells. *J. Neurochem.* **54**, 1812–1815
22. De Silvestris, M., D'Arrigo, A., and Borgese, N. (1995) The targeting information of the mitochondrial outer membrane isoform of cytochrome b_5 is contained within the carboxyl-terminal region. *FEBS Letters* **370**, 69–74
23. Alberati-Giani, D., Cesura, A.M., Broger, C., Warren, W.D., Rover, S., and Malherbe, P. (1997) Cloning and functional expression of human kynurenine 3-monooxygenase. *FEBS Letters* **410**, 407–412
24. Han, Q., Calvo, E., Marinotti, O., Fang, J., Rizzi, M., James, A., and Li, J. (2003) Analysis of the wild-type and mutant genes encoding the enyme kynurenine monooxygenase of the yellow fever mosquito, *Aedes aegypti*. *Insect Mol. Biol.* **12**, 483–490
25. Hirai, M., Kluchi, M., Wang, J., Ishii, A., and Matsuoka, H. (2002) cDNA cloning, functional expression and characterization of kynurenine 3-hydroxylase of *Anopheles stephensi* (Diptera: Culicidae). *Insect Mol. Biol.* **11**, 497–504
26. Kozak, M (1984) Point mutations close to the AUG initiator codon affect the efficiency of translation of rat preproinsulin in vivo. *Nature* **308**, 241–246
27. Weijer, W.J., Hofsteenge, J., Beintema, J.J., Wierenga, R.K., and Drenth, J. (1983) *p*-Hydroxybenzoate hydroxylase from *Pseudomonas fluorescens* 2. Fitting of the amino-acid sequence to the tertiary structure. *Eur. J. Biochem.* **133**, 109–118
28. Schreuder, H.A., Prick, P.A., Werenga, R.K., Vriend, G., Wilson, K.S., Hol, W.G., and Drenth, J. (1989) Crystal structure of the *p*-hydroxybenzoate hydroxylase-substrate complex refined at 1.9Å resolution. Analysis of the enzyme-substrate and enzyme-product complexes. *J. Mol. Biol.* **208**, 879–896
29. Borgese, N., Colombo, S., and Pedrazzini, E. (2003) The tale of tail-anchored proteins: coming from the cytosol and looking for a membane. *J. Cell Biol* **161**, 1013–1019
30. Borgese, N., Brambillasca, S., and Colombo, S (2007) How tails guide tail-anchored proteins to their destinations. *Curr. Opin. Cell Biol.* **19**, 368–375
31. Chen, K., Wu, H-F., and Shih, C. (1996) Influence of C terminus on monoamine oxidase A and B catalytic activity. *J. Neurochem.* **66**, 797–803
32. Hayaishi, O. (1962) Kynurenine Hydoxylase, Methods *Enzymol.* **5**, 807–809
33. Mitoma, J. and Ito, A. (1992) Mitochondrial targeting signal of rat liver monoamine oxidase B is located at its carboxy terminus. *J. Biochem.* **111**, 20–24
34. Kuroda, R., Ikenoue, T., Honsho, M., Tsujimoto, S., Mitoma, J., and Ito, A. (1998) Charged amino acids at the carboxyl-terminal portions determine the intracellular locations of two isoforms of cytochrome b_5. *J. Biol. Chem.* **273**, 31097–31102
35. Habib, S.J., Vasiljev, A., Neupert, W., and Rapaport, D. (2003) Multiple functions of tail-anchor domains of mitochondrial outer membrane proteins. *FEBS Letters* **555**, 511–515
36. Bereiter-Hahn, J. (1990) Behavior of mitochondria in the living cell. *Int. Rev. Cytol.* **122**, 1–63
37. Pedrazzini, E., Villa, A., and Borgese, N. (1996) A mutant cytochorme b_5 with a lengthened membrane anchor escapes from the endoplasmic reticulum and

reaches the plasma membrane. *Proc. Natl Acad. Sci.* **93**, 4207–4212
38. Borgese, N., Gazzoni, I., Barberi, M., Colombo, S., and Pedrazzini, E. (2001) Targeting of a tail-anchored protein to endoplasmic reticulum and mitochondrial outer membrane by independent but competing pathways. *Mol. Biol. Cell* **12**, 2482–2496
39. Shiao, Y.-J., Balcerzak, B., and Vance, J.E. (1998) A mitochondrial membrane protein is required for translocation of phosphatidylserine from mitochondria-associated membranes to mitochondria. *Biochem. J.* **331**, 217–223
40. Vance, J.E., Stone, S.J., and Faust, J.R. (1997) Abnormalities in mitochondria-associated membranes and phospholipid biosynthetic enzymes in the mnd/mnd mouse model of neuronal ceroid lipofuscinosis. Biochim. *Biophys. Acta.* **1344**, 286–299
41. Aithal, H.N., Janki, R.M., Gushulak, B.D., and Tustanoff, E.R. (1976) Lipid-protein interactions in the outer membranes of yeast and rat liver mitochondria. *Arch. Biochem. Biophys.* **176**, 1–11
42. Lewin, B. (2000) Protein Synthesis. Small subunits scan for initiation sites on eukaryotic mRNA in *Genes VII* (Lewin, B., ed.), pp. 149–152, Oxford University Press, Oxford
43. Danpure, C.J. (1995) How can the products of a single gene be localized to more than one intracellular compartment? *Trends Cell Biol.* **5**, 230–238
44. Banerjee, R. and Zou, C.-G. (2005) Redox regulation and reaction mechanism of human cystathionine-β-synthase: a PLP-dependent hemesensor protein. *Arch. Biochem. Biophys.* **433**, 144–156
45. Crozier, K.R. and Moran, G.R. (2007) Heterologous expression and purification of kynurenine-3-monooxygenase from *Pseudomonas fluorescens* strain 17400. *Protein Express. Purific.* **51**, 324–333
46. Eisenberg, D. (1984) Three-dimensional structure of membrane and surface proteins. *Ann. Rev. Biochem.* **53**, 595–623
47. Pellicciari, R., Amori, L., Costantino, G., Giordani, A., Macchiarulo, A., Mattoli, L., Pevarello, P., Speciale, C., and Varasi, M. (2003) Modulation of the kynurenine pathway of tryptophan metabolism in search for neuroprotective agents, focus on kynurenine-3-hydroxylase in *Advances in Experimental Medicine and Biology*, Vol. 527, Developments in Tryptophan and Serotonin Metabolism (Allegri, G., Costa, C.V.L., Ragazzi, E., Steinhart, H., and Varesio, L., eds.), pp. 621–628, Kluwer Academic/Plenum Publishers, NY
48. Entsch, B. and Van Berkel, W.J.H. (1995) Structure and mechanism of para-hydroxybenzoate hydroxylase. *FASEB J.* **9**, 476–483
49. Binda, C., Hubalek, F., Li, M., Edmondson, D.E., and Mattevi, A. (2004) Crystal structure of human monoamine oxidase B, a drug target enzyme monotopically inserted into the mitochondrial outer membrane. *FEBS Letters* **564**, 225–228
50. Rapaport, D. (2003) Finding the right organelle. Targeting signals in mitochondrial outer-membrane proteins. *EMBO Reports* **4**, 948–952
51. Pedrazzini, E., Villa, A., Longhi, R., Bulbarelli, A., and Borgese, N. (2000) Mechanism of residence of cytochrome *b*(5), a tail-anchored protein, in the endoplasmic reticulum. *J. Cell Biol* **148**, 899–931
52. Isenmann, S., Khew-Goodall, Y., Gamble, J., Vadas, M., and Wattenberg, B.W. (1998) A splice-isoform of vesicle-associated membrane protein-1 (VAMP-1) contains a mitochondrial targeting signal. *Mol. Biol. Cell* **9**, 1649–1660
53. Kaufmann, T., Schlipf, S., Sanz, J., Neubert, K., Stein, R., and Borner, C. (2003) Characterization of the signal that directs Bcl-x_L, but not Bcl-2, to the mitochondrial outer membrane. *J. Cell Biol* **160**, 53–64